Materials Research Proceedings 44 (2024) 393-401 https://doi.org/10.21741/9781644903254-43

The role of thermomechanical processing in controlling the microstructure inhomogeneity as a way to create special properties of $(FeMnNiCo)_{1-x}$ Mo_x high entropy alloy - a practical approach

CICHOCKI Kamil[1,a *], BAŁA Piotr[1,b], HENSCHEL Sebastian[2,c], KRÜGER Lutz[2,d] and MUSZKA Krzysztof[1,f]

[1]AGH University of Krakow, Department of Metal Forming, and Metallurgical Engineering, al. A. Mickiewicza 30, 30-059 Kraków, Poland

[2]TU Bergakademie Freiberg, Institute of Materials Engineering, Gustav-Zeuner-Str. 5, 09599 Freiberg, Germany

[a]cichocki@agh.edu.pl, [b]pbala@agh.edu.pl, [c]sebastian.henschel@iwt.tu-freiberg.de, [d]krueger@ww.tu-freiberg.de, [e]muszka@agh.edu.pl

Keywords: High Entropy Alloy, Strain Rate Effect, Temperature Effect, Compression Test, Strain Hardening, Microstructure, Twinning

Abstract. From modern alloys, increasingly demanding combinations of properties are expected, enabling their use as structural materials in new areas of application such as the energy industry (Liquid Natural Gas and hydrogen tanks), military, or space. One of the fundamental expectations for constructional materials used in these sectors is high energy absorption capacity while maintaining high strength (often at low temperatures where e.g. conventional steels exhibit brittleness). Simultaneously, they require appropriate plastic deformation susceptibility (formability) and other additional parameters (e.g., corrosion resistance, weldability, fatigue resistance). Designing manufacturing technologies for the metal forming of structural elements from modern engineering materials for the aforementioned applications requires a holistic approach and understanding of the relationships between process parameters (time, temperature, deformation, strain rate), microstructural phenomena (recovery/strengthening mechanisms, phase transformations, precipitation processes), and resulting properties (strength, ductility, toughness). In this work I will provide a practical example of designing specific properties of $(CoNiFeMn)_{1-x}Mo_x$ high entropy alloys by controlling microstructure development at each stage of the metal forming process. The role of recrystallisation, grain growth, and the precipitation of the phase in controlling grain size - a key parameter defining the susceptibility to twinning/nanotwinning in this alloy at cryogenic temperatures - will be discussed.

Introduction

High-entropy alloys are a family of alloys that has been intensively studied over the last few years. The first alloy was the so-called Cantor alloy with an equilibrium chemical composition[1]. These alloys are characterised by four effects: slow diffusion, cocktail effect, high entropy and lattice distortion[2]. Further research has shown that high-entropy alloys have a number of unique properties such as, low stacking fault energy, very good mechanical properties at cryogenic conditions.

The susceptibility to hot deformation in high-entropy alloys has been studied over recent years. These studies mainly concern alloys in the FCC lattice. Studies for Cantor alloys have shown that high-entropy alloys are characterised by a relatively high activation energy of dynamic recrystallisation [3]. Studies have shown that the addition of molybdenum increases the activation energy of recrystallisation in the $CrFeCoNiMo_{0.3}$ alloy [4]. Investigating the possibility of

deforming these alloys by twinning is also a popular research direction. Kaushik [5] showed that Cantor's alloy tends to deform by twinning during cold rolling.

This paper presents a scheme for the preparation, in terms of microstructure, of high-entropy alloys of composition $(CoNiFeMn)_{1-x}Mo_x$ for mechanical testing under cryogenic conditions at high strain rates. The desired initial microstructure was achieved by hot deformation analysis, cold rolling and appropriate heat treatment.

Materials and Methods

Ingots were prepared in a VIM LAB 20-50 type induction vacuum furnace and cast in a controlled atmosphere. For the study, ingots of 1 kg were prepared for three alloys with the following chemical compositions CoNiFeMn, $(CoNiFeMn)_{95}Mo_5$ and $(CoNiFeMn)_{90}Mo_{10}$.

The ingots were then hot forged into flat bars at 1150° C using a 500T ZAMET servo-hydraulic press. The initial microstructure for the compression tests is shown in Figure 1. Microstructure analysis was performed after heating to 1150°C and holding for 300 s.

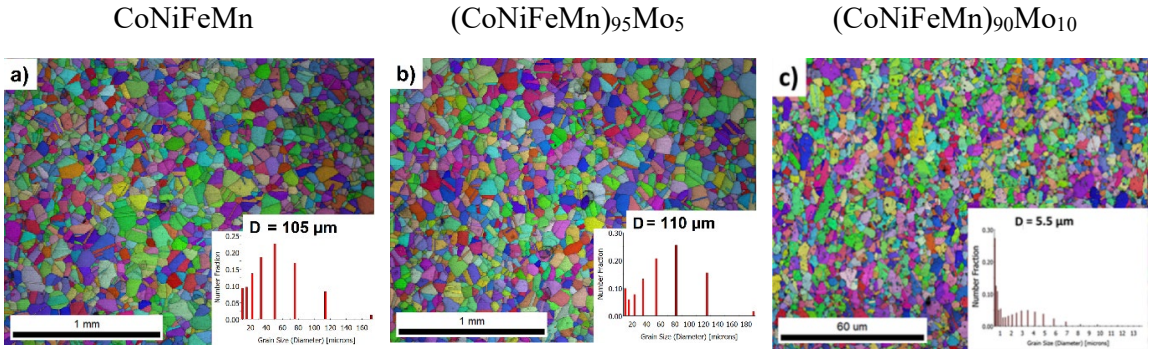

Fig. 1. Initial microstructure for compression tests of the tested alloys.

Grain size measurements were made after the annealing twins were removed. The materials are characterised by a stable solid solution in the FCC lattice. The significantly smaller grain size for the alloy $(CoNiFeMn)_{90}Mo_{10}$ is due to the presence of the intermetallic μ phase, which limits grain growth [6].

Methods. Compression tests were performed on an ASP servo-hydraulic thermomechanical simulator equipped with an induction furnace. Cylindrical specimens measuring 8x8 mm were prepared for compression tests. The specimens were cut from pre-plasticised material. The specimens were heated at a rate of 5°C/s to a temperature of 1150°C and held for 300 s. The choice of temperature was dictated by the fact that materials oxidise rapidly at higher temperatures. Then cooled at a cooling rate of 4°C/s to the deformation temperature. Deformation was carried out at temperatures of 900° C, 1000° C, 1100°C with strain rates of 0.1 s^{-1} , 1 s^{-1} , 10 s^{-1} . The final strain was set at 0.7 of the true strain. A more accurate analysis of the hot deformation behaviour of the materials can be based on the determination of the deformational consolidation:

$$\theta = \frac{d\sigma}{d\varepsilon} \tag{1}$$

The method of Najafizadeh and Jonas was used to determine the values of stress σ_C and strain ε_C critical [7]. The critical stress is determined from a third-degree polynomial function in θ - σ, determined from zero to the peak stress value according to equation:

$$\theta = A\sigma^3 + B\sigma^2 + C\sigma + D \tag{2}$$

where: A, B, C, D - are constants. The second derivative of Eq. 2 as a function of σ can be written as:

$$\frac{d^2\theta}{d\sigma^2} = 6A\sigma + 2B \tag{3}$$

The critical stress can be determined at point $\frac{d^2\theta}{d\sigma^2} = 0$. Then:

$$6A\sigma + 2B = 0 \rightarrow \sigma_C = \frac{-B}{3A} \tag{4}$$

Cold rolling was carried out on a laboratory 4-high mill with a working roll diameter of 100 mm.

SEM/EBSD analysis was performed on a FEI Nova NanoSEM 450 scanning microscope (SEM) (STEM) using an EDAX EBSD Velocity detector. The specimens were prepared by grinding and mechanical polishing. EBSD analysis was performed in the centre of the compressed sample, with an accelerating voltage of 20 kV, a spot size of 6 and a step of 0.5 μm. The processing of the obtained results was performed in OIM-TSL 8 software.

Results and Discussion

The resulting flow curves for the tested high-entropy tested, obtained at different temperatures and strain rates, are shown in Fig. 2. During hot deformation of the material, the characteristic plateau is the result of the phenomenon of recovery (DRV) whereas the flow softening results from occurrence of the dynamic recrystallisation (DRX).

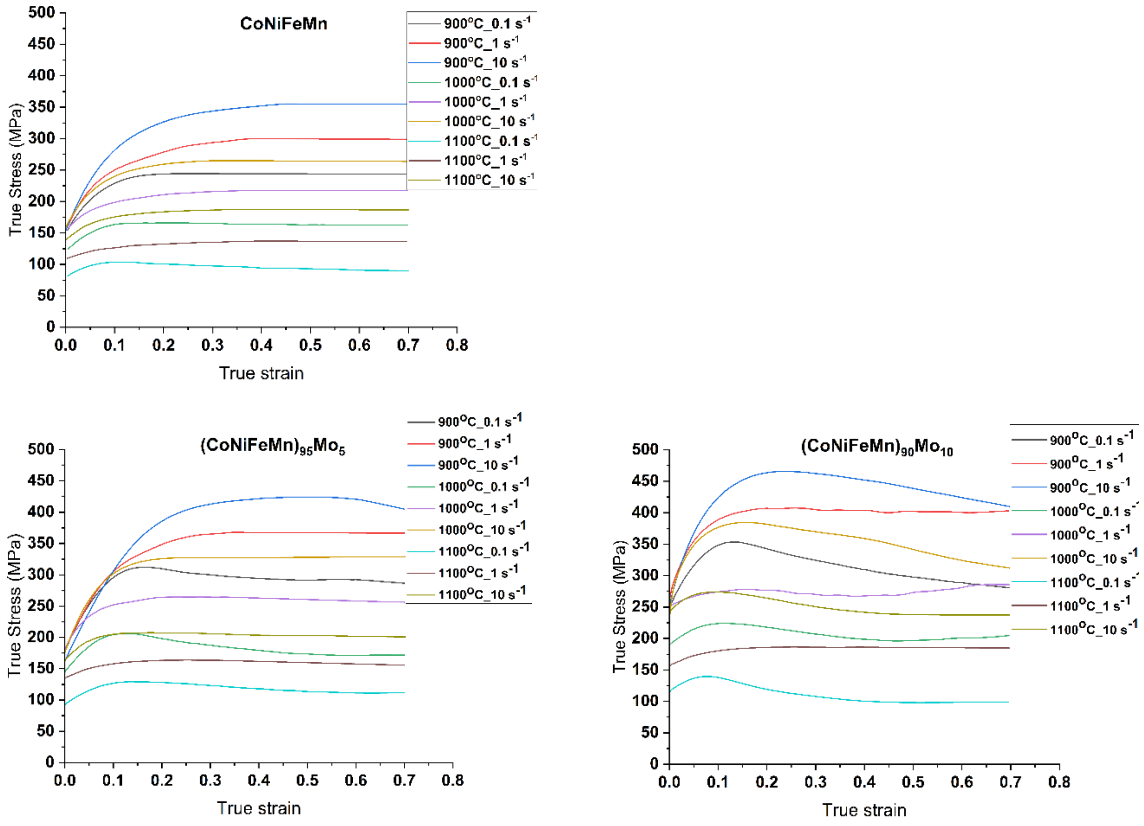

Fig. 2. Flow curves for the high-entropy alloys tested.

From the obtained flow curves it can be seen that, the addition of molybdenum causes an increase in flow stress. Comparing CoNiFeMn and $(CoNiFeMn)_{95}Mo_5$ alloys, this increase is mainly due to solution strengthening, due to the similar grain size of the materials studied. In the case of the $(CoNiFeMn)_{90}Mo_{10}$ alloy, the increase in stress is additionally due to the presence of the μ-phase precipitates, which cause the effect of precipitation strengthening. It should also be noted that with the addition of molybdenum the peak deformation as well as the subsequent softening is much more pronounced.

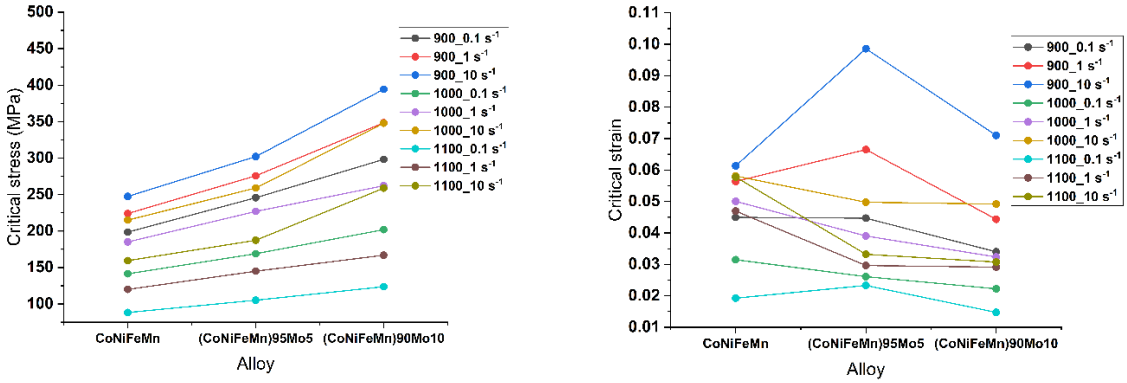

Fig. 3. a) critical stress, b) critical strain.

Analysing the results obtained for critical and peak stress, the stress values increase with the addition of molybdenum. In the case of critical stress values, the strongest, inter-alloy relationship is observed at 900°C. At 1100°C the relationship is linear. In the case of critical strain values at 900° C in the alloy $(CoNiFeMn)_{95}Mo_5$ there is an increase in critical strain values, followed by a decrease in $(CoNiFeMn)_{90}Mo_{10}$. This phenomenon may be due to a strain-induced precipitation process where, as will be discussed in the following sections, in the case of the deformed material, μ-phase precipitates appear at the temperatures up to 1000°C [8]. The observation of a decrease in critical strain confirms that the addition of molybdenum promotes the occurrence of dynamic recrystallisation, occurring earlier. Comparing CoNiFeMn and $(CoNiFeMn)_{95}Mo_5$ alloys this is also due to the fact that molybdenum reduces the stacking fault energy which favours the occurrence of DRX. In the $(CoNiFeMn)_{90}Mo_{10}$ alloy there are additionally μ-phase precipitation in the temperature range of hot forming. The larger decrease in strain values is due to the higher stored energy associated with the additional separation strengthening. Another aspect is the grain size, which is much smaller compared to other alloys. A smaller grain size, increases the volume of grain boundaries, which are privileged nucleation sites for new grains which means that dynamic recrystallisation can start at lower strains. In addition, the smaller grain size increases the proportion of strengthening from the grain boundaries, which also translates into a shift in the onset of recrystallisation towards smaller strains.

The activation energies of dynamic recrystallisation were determined from the slope factor of the linear function at ln(sinh(ασp)) - 1000/T. The values are included in the graphs in Fig. 4.

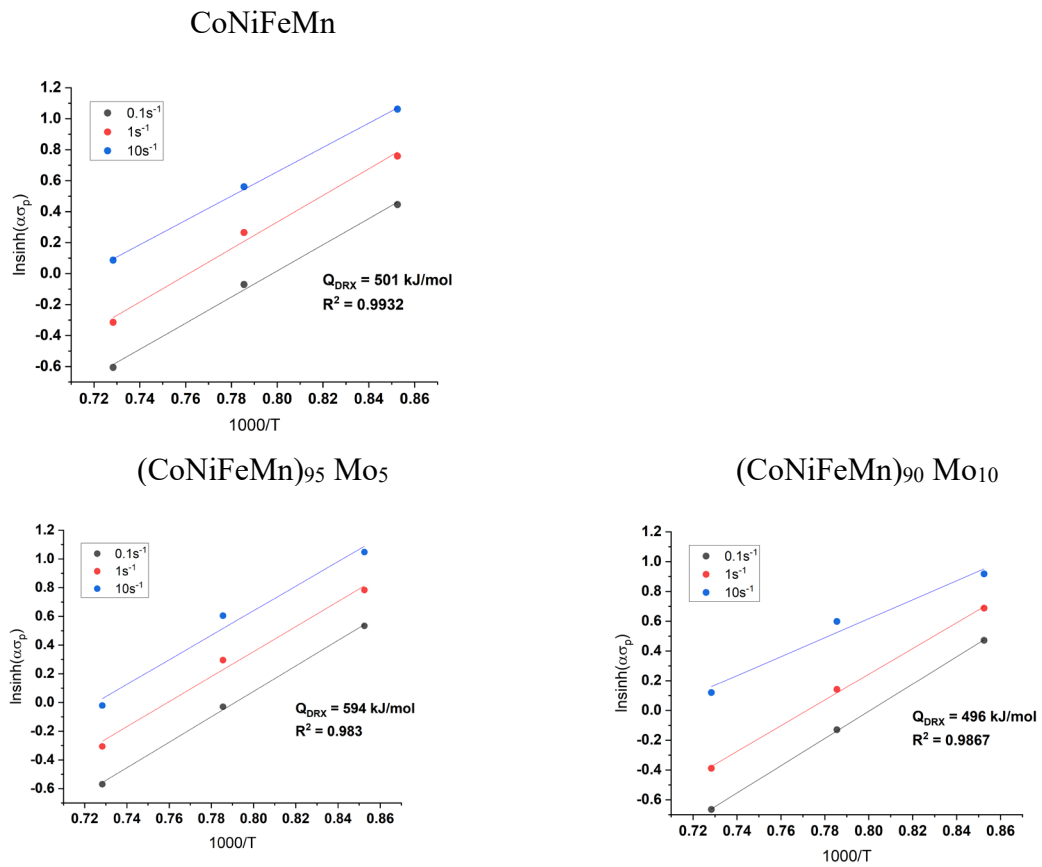

Fig. 4. Activation energy of dynamic recrystallisation for the alloys studied.

The above analysis shows that the addition of molybdenum increases the activation energy of dynamic recrystallisation. For alloys containing pure FCC solid solution, the addition of 5% atomic molybdenum results in an increase in Q_{DRX} of 93 kJ/mol. The decrease in Q_{DRX} values is dictated by the previously described effects from the existing precipitates as well as the smaller grain size. The values obtained are comparable to those obtained for other high-entropy alloys[3][9]. High values of activation energies, close to or slightly higher than the diffusion activation energies of the individual elements, indicate the effect of sluggish diffusion and hinder the occurrence of diffusion processes such as dynamic recrystallisation [10][11].

Investigations into the behaviour of materials at elevated temperatures made it possible to design the hot-rolling process and prepare the material accordingly for subsequent cold rolling.

Cold rolling, microstructure evolution. The hot-rolling process parameters were developed based on the results obtained on the ASP thermomechanical simulator. The materials were plastically processed according to the scheme shown in Fig. 5. The total given strain was 0.74. The material was then relaxed and cooled in air. The relaxation allowed the completion of the meta-dynamic and static recrystallisation processes. The selection of appropriate process parameters allowed the material to be fully recrystallised, with equiaxial grains, and with the characteristic annealing twins present (Fig. 5).

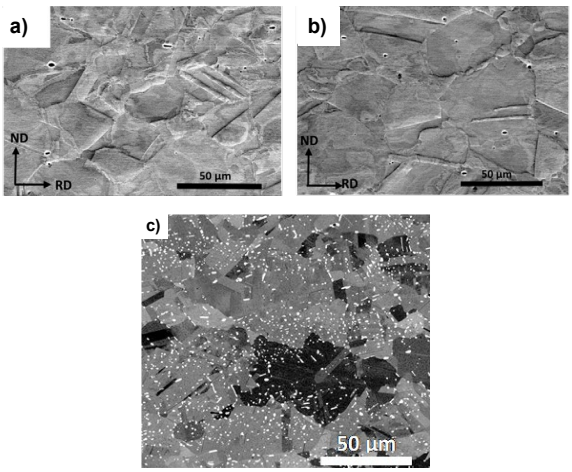

Fig. 5. SEM-BSE microstructure images after hot rolling of (a) CoNiFeMn, (b) (CoNiFeMn)95Mo5, (c) (CoNiFeMn)90Mo10 alloys.

By analysing the microstructures, it can be seen that the (CoNiFeMn)90Mo10 alloy exhibits μ-phase precipitates with varying morphologies. In addition, there are small areas free of precipitates in the microstructure (Fig. 5c). This may be due to the fact of uneven deformation during hot rolling, as well as the occurrence of a heat dissipation gradient during cooling. The microstructure photographs show the initial microstructure for cold rolling. The final actual deformation was taken as ε = 0.7. Fig. 6 shows the IPF after cold rolling after various deformations for the tested materials.

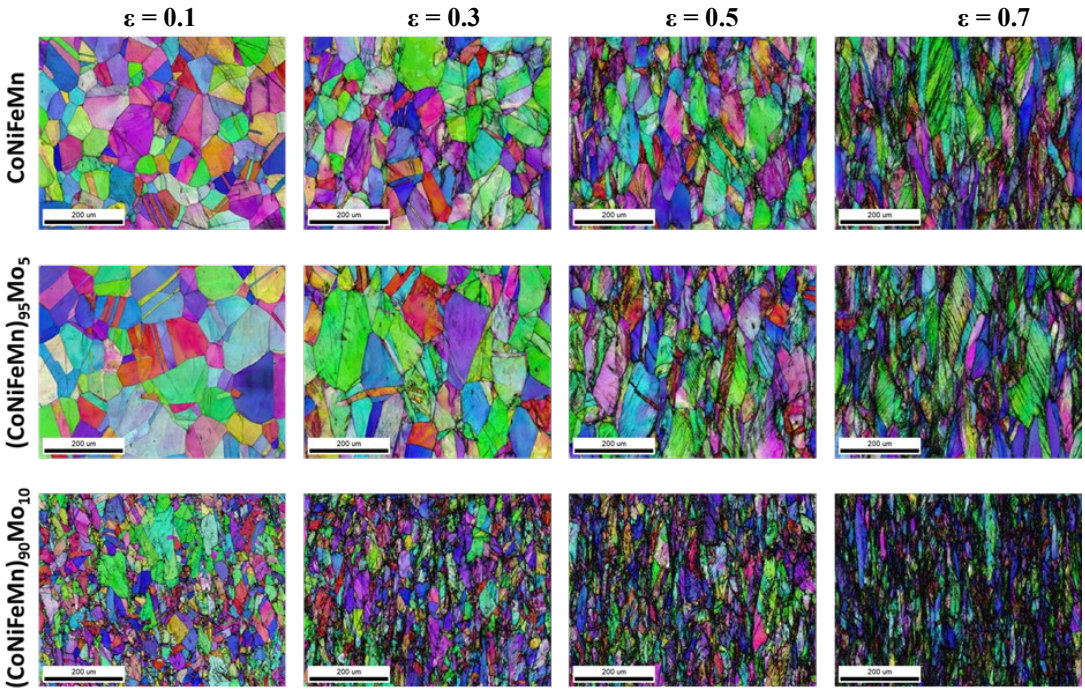

Fig. 6. IPF maps obtained by EBSD analysis after cold rolling with different degrees of deformation.

In the microstructure after deformation ε = 0.1, it is still possible to observe equiaxial grains with visible annealing twins. In this case, the difference in grain size between the materials can be seen. In the alloys CoNiFeMn and $(CoNiFeMn)_{95}Mo_5$, the grain size is similar. In the case of the $(CoNiFeMn)_{90}Mo_{10}$ alloy, the grain size is smaller as a result of the blocking of grain growth after

hot forming by μ-phase precipitation. The beginning of substructure formation can be observed, suggesting the appearance of low angle grain boundaries (LAB). After deformation ε = 0.3, the grains begin to elongate in the rolling direction. Increasing the degree of deformation also increases the number of low angle grain boundaries. The microstructure after a strain of 0.5 is already characterised by elongated grains in the rolling direction. The microstructure of the alloy $(CoNiFeMn)_{90}Mo_{10}$ already reveals thick bands extending along the rolling direction. The formation of a band structure begins. For the other materials, these microstructural phenomena occur at strain ε = 0.7. In addition to the high- and low-angle grain boundaries, the appearance of strain twins was observed in the microstructure (Fig. 7). At strain ε = 0.1, annealing twins are still visible. Deformation twins appear in the CoNiFeMn alloy at a strain of ε = 0.7. In the case of the alloy $(CoNiFeMn)_{95}$ Mo_5 twins can already be observed at lower strains.

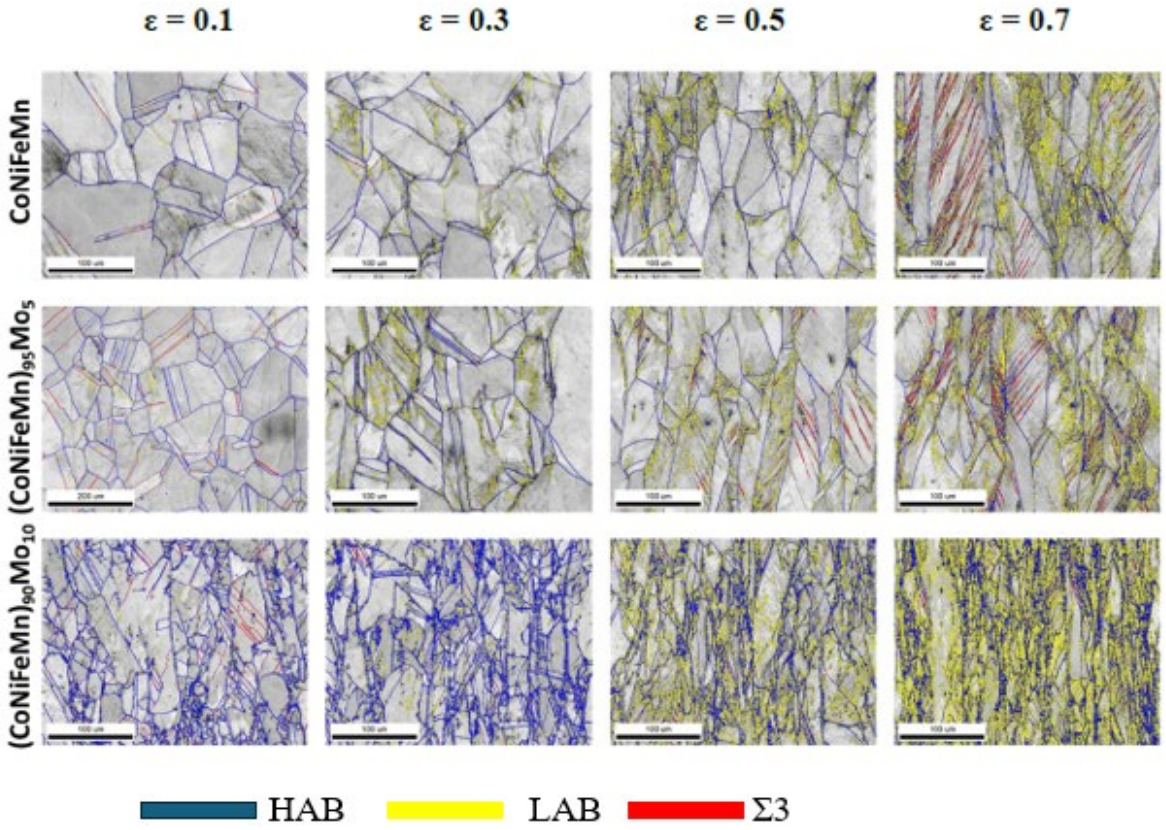

Fig. 7. High-angle, low-angle and twin boundaries evolution during deformation progresses.

The presence of twins is also confirmed by the linear disorientation measurement presented in Fig. 8. The linear disorientation measurement was performed inside the grain in the <110> direction. From the analysis presented in the graph, increase in disorientation up to 60° can be observed, which confirms the rotation of the crystal during deformation and thus indicates the appearance of deformation twins.

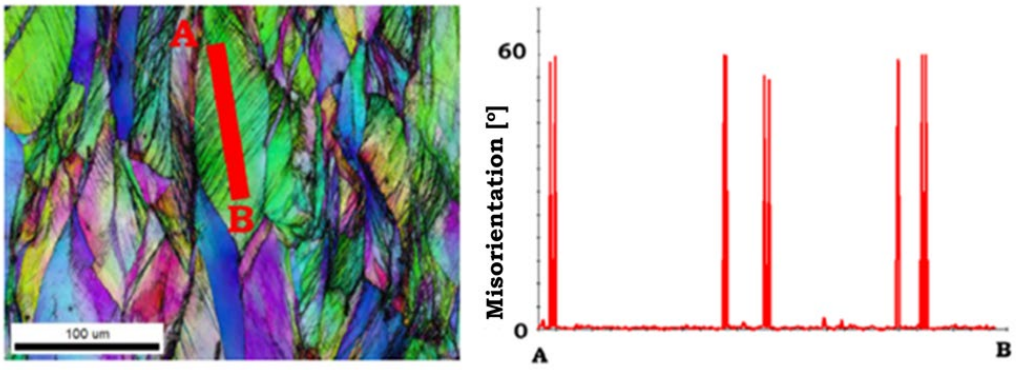

Fig. 8. Linear grain disorientation in the <110> direction.

Static recrystallisation and grain growth after cold rolling is therefore a very important factor in controlling the ability to absorb the impact energy through twinning mechanism. A detailed analysis of the static recrystallisation process and grain growth has been discussed in detail in our previous work [8]. Fig. 9 shows the grain size as a function of temperature after cold rolling.

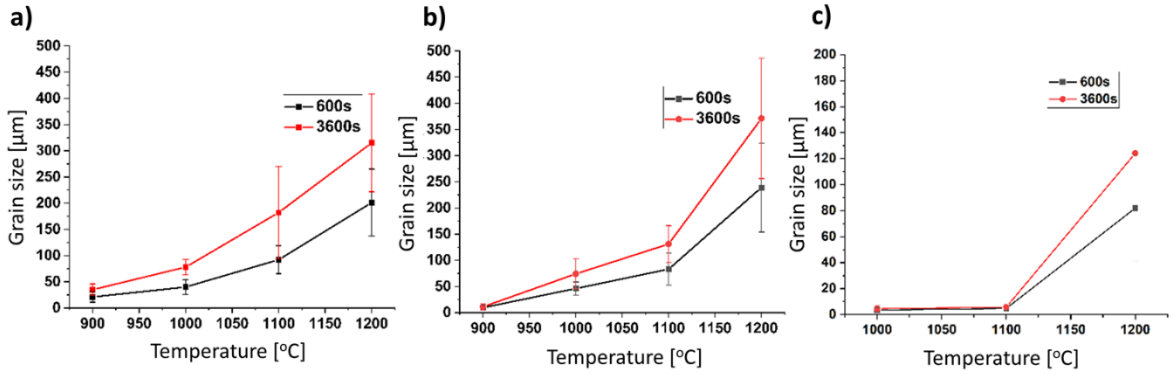

Fig. 9. a) CoNiFeMn [8], (b) $(CoNiFeMn)_{95}Mo_5$ [8], (c) $(CoNiFeMn)_{90}Mo_{10}$.

Based on the presented research it can be concluded that by knowing the mechanisms controlling the grain size both during hot and cold deformation, makes it possible to prepare a material with a suitable microstructure for possible applications under both quasi-static or dynamic load–bearing applications – especially at low temperature where nano-twinning and twinning is expected as a main mechanism that increasing the toughness of these new group of materials.

Summary

In this study, the hot deformation behaviour of the proposed alloys was studied, as well as the microstructure evolution during cold rolling and heat treatment. Based upon the presented research, the following conclusion can be drawn:

- The addition of 5% molybdenum to the CoNiFeMn alloy increases the activation energy of dynamic recrystallisation. In the alloy with 10% Mo, the DRX activation energy is lower due to the increased energy accumulated by the smaller grain size and the presence of µ-phase precipitates.
- The evolution of the microstructure after rolling shows that strain twins can be observed in the alloy with 5% Mo at lower strains than in the alloy without Mo. This demonstrates the reduction of alignment error energies by the addition of Mo to the alloy.

Acknowledgement

Research project supported by the program “Excellence initiative—research university” from the AGH University of Krakow is acknowledged.

References

[1] B. Cantor, I.T.H. Chang, P. Knight, A.J.B. Vincent, Microstructural development in equiatomic multicomponent alloys, Mater. Sci. Eng. A 375-377 (2004) 213-218. https://doi.org/10.1016/j.msea.2003.10.257

[2] D. B. Miracle, High-Entropy Alloys: A Current Evaluation of Founding Ideas and Core Effects and Exploring 'Nonlinear Alloys, JOM 69 (2017) 2130-2136. https://doi.org/10.1007/s11837-017-2527-z

[3] J.M. Park, J. Moon, J.W. Bae, M.J. Jang, J. Park, S. Lee, H.S. Kim, Strain rate effects of dynamic compressive deformation on mechanical properties and microstructure of CoCrFeMnNi high-entropy alloy, Mater. Sci. Eng. A 719 (2018) 155-163. https://doi.org/10.1016/j.msea.2018.02.031

[4] J. Wang, Y. Liu, B. Liu, Y. Wang, Y. Cao, T. Li, R. Zhou, Flow behaviour and microstructures of powder metallurgical CrFeCoNiMo0.2 high entropy alloy during high temperature deformation, Mater. Sci. Eng. A 689 (2017) 233-242. https://doi.org/10.1016/j.msea.2017.02.064

[5] L. Kaushik, M.-S. Kim, J. Singh, J.-H. Kang, Y.-U. Heo, J.-Y. Suh, S.-H. Choi, Deformation mechanisms and texture evolution in high entropy alloy during cold rolling, Int. J. Plast. 141 (2021) 102989. https://doi.org/10.1016/j.ijplas.2021.102989

[6] K. Cichocki, P. Bała, T. Kozieł, G. Cios, N. Schell, K. Muszka, Effect of Mo on Phase Stability and Properties in FeMnNiCo High-Entropy Alloys, Metall. Mater. Trans. A Phys. Metall. Mater. Sci. 53 (2022) 1749-1760. https://doi.org/10.1007/s11661-022-06629-x

[7] A. Najafizadeh, J.J. Jonas, Predicting the critical stress for initiation of dynamic recrystallization, ISIJ Int. 46 (2006) 1679-1684. https://doi.org/10.2355/isijinternational.46.1679

[8] K. Cichocki, P. Bała, M. Kwiecień, M. Szymula, K. Chrzan, C. Hamilton, The influence of Mo addition on static recrystallization and grain growth behaviour in CoNiFeMn system subjected to prior deformation, Arch. Civ. Mech. Eng. 24 (2024). https://doi.org/10.1007/s43452-024-00888-8

[9] S.A. Sajadi, M.R. Toroghinejad, A. Rezaeian, G.R. Ebrahimi, Dynamic recrystallization behavior of the equiatomic FeCoCrNi high-entropy alloy during high temperature deformation, J. Mater. Res. Technol. 20 (2022) 1093-1109. https://doi.org/10.1016/j.jmrt.2022.07.055

[10] W. Kucza, J. Dąbrowa, G. Cieślak, K. Berent, T. Kulik, M. Danielewski, Studies of 'sluggish diffusion' effect in Co-Cr-Fe-Mn-Ni, Co-Cr-Fe-Ni and Co-Fe-Mn-Ni high entropy alloys; determination of tracer diffusivities by combinatorial approach, J. Alloy. Compd. 731 (2018) 920-928. https://doi.org/10.1016/j.jallcom.2017.10.108

[11] K.Y. Tsai, M.H. Tsai, J.W. Yeh, Sluggish diffusion in Co-Cr-Fe-Mn-Ni high-entropy alloys, Acta Mater. 61 (2013) 4887-4897. https://doi.org/10.1016/j.actamat.2013.04.058